

## Electron detachment from anions in aqueous solutions studied by two- and three-pulse femtosecond spectroscopy\*

Hristo Iglev, Martin K. Fischer, and Alfred Laubereau<sup>‡</sup>

*Department of Physics, Technical University of Munich, James-Franck-Strasse, D-85748 Garching, Germany*

**Abstract:** The electron photodetachment of the aqueous halides and hydroxide is studied after resonant excitation in the lowest charge-transfer-to-solvent (CTTS) state. The initially excited state is followed by an intermediate assigned to a donor-electron pair that displays a competition of recombination and separation. Using pump–repump–probe (PREP) spectroscopy, the pair species is verified via a secondary excitation with separation of the pairs so that the yield of released electrons is increased. The observed recombination process on the one hand and the similar absorptions of the intermediate and the hydrated electron on the other hand suggest that the donor-electron pairs incorporate only few if not just one water molecule. The geminate dynamics measured in the various CTTS systems reveal a strong influence of the parent radical. The electron survival probability decreases significantly from 0.77 to 0.29 going from F<sup>−</sup> to OH<sup>−</sup>. The extracted dissociation rates of the halogen-electron pairs seem to be proportional to the mutual diffusion coefficients of the geminate particles, while such a relation between the recombination rate and the diffusion coefficient is not found. Results for I<sup>−</sup> show that excitation of a higher-lying CTTS state opens a new relaxation channel, which directly leads to a fully hydrated electron, while the relaxation channel discussed above is not significantly affected.

**Keywords:** aqueous solutions; charge-transfer-to-solvent (CTTS) transitions; photo-detachment; solvated electrons; time-resolved spectroscopy.

### INTRODUCTION

Photoinduced electron detachment from aqueous inorganic anions is a simple example for solvent-mediated electron transfer [1]. The process proceeds through charge-transfer-to-solvent (CTTS) states [2,3]. Computer simulations [4] show that the spatially extended CTTS wave function overlaps with solvent intervals that may serve as pre-traps for the excess electron. In this way, the electron can be efficiently transferred to the solvent. The calculations predict that the released electron is embedded by solvent molecules close to the parent radical, forming a weakly bound donor-electron pair [5–8]. Femtosecond pump–probe spectroscopy on various CTTS systems supports the predicted formation of pair species [9–17]. The extracted depth of the potential well is typically in the order of a few  $k_{\text{B}}T$  [15–19]. The quantum yield of long-lived solvated electrons increases monotonically for higher photon

\*Paper based on a presentation at the 31<sup>st</sup> International Conference on Solution Chemistry (ICSC-31), 21–25 August 2009, Innsbruck, Austria. Other presentations are published in this issue, pp. 1855–1973.

<sup>‡</sup>Corresponding author

energies of the excitation process [18]. The phenomenon is assigned to an additional detachment channel with direct ejection of electrons [5,6].

The direct verification of the halogen-electron pair and the detailed investigation of its properties are missing, since the latter displays spectral features very similar to those of the hydrated electron [7,8]. In the present work, we report on electron photodetachment of aqueous  $F^-$ ,  $Cl^-$ ,  $Br^-$ ,  $I^-$ , and  $OH^-$  after excitation with 8.0, 6.4, 6.15, 5.1, and 6.15 eV, respectively. In this way, a resonant excitation in the lowest CTTS state of the corresponding anion is achieved [2,3,20,21]. In spite of the similar excitation conditions, the relaxation dynamics measured in the absorption maximum of the hydrated electron varies significantly for different anions. To elucidate this phenomenon in more detail, the photodetachment process is studied by pump–repump–probe (PREP) spectroscopy [22]. The technique offers an elegant way for studying the electron transfer mechanism [23,24]. Re-excitation of the excess electron was reported to hinder its recombination with the donor, leading to a significant increase of the long-time survival of solvated electrons [22,25,26]. The PREP data measured in aqueous bromide solution give experimental evidence for the formation of donor-electron pairs separated most likely by only a few if not just one water molecule. The dissociation and recombination rates of the pair are compared with the mutual diffusion coefficient of the geminate particles.

## EXPERIMENTAL

The pump–probe data presented below are performed by three different laser systems. The two-photon excitation experiments in aqueous fluoride are conducted with the help of a colliding pulse mode-locked (CPM) dye laser system [21]. This system produces 620-nm pulses of 150  $\mu J$  and 110 fs at a repetition rate of 50 Hz. A portion of the amplified laser pulse is frequency-doubled in a 100- $\mu m$  BBO-crystal. Pulses with energy of up to 10  $\mu J$  and 175 fs duration are obtained at 310 nm (4.0 eV). The UV pulses are used for two-photon electron detachment of aqueous fluoride solution, while the absorption changes induced in the sample are monitored in a broad spectral range from 450 to 1050 nm. The relative polarization of the pump and probe beams are set to the magic angle of 54.7° (for all samples discussed below).

The measurements in aqueous chloride and iodide are performed with a Ti:sapphire amplifier system yielding 775-nm pulses of 800- $\mu J$  pulses and 150 fs with 1 kHz repetition rate [18]. For the single-photon excitation process, pulses at 194 nm (6.4 eV) and 242 nm (5.1 eV) were used. The 194-nm pulses (energy of 0.7  $\mu J$  and duration of 700 fs) are achieved by fourth harmonic generation of the fundamental laser at 775 nm [27]. To generate the 242-nm signal, the output of a non-collinear optical parametric amplifier was tuned to 484 nm and frequency-doubled in a 100- $\mu m$  BBO-crystal providing pulses with energy of 1  $\mu J$  and duration of 100 fs [18]. The relaxation dynamics are monitored by probing pulses in the range from 350 to 1100 nm derived from a white-light continuum.

For the electron photodetachment with UV photons at 202 nm in aqueous bromide, iodide, and hydroxide we use a home-built Ti:sapphire laser system delivering 90 fs pulses at 810 nm and 1 kHz repetition rate [22]. The solvated electrons are generated by linear absorption of the fourth harmonic (pulses of 1  $\mu J$  and 180 fs).

The secondary excitation of the intermediates and/or fully detached electrons is achieved by single-photon absorption at 810 nm induced by a fraction of the laser pulse at low intensity level. The corresponding PREP-signal  $\Delta(\Delta OD)$  discussed below represents the probe absorption change induced by the repump pulse relative to the pump–probe signal, i.e., the difference of probe absorption changes measured after two-pulse excitation (pump and repump) and for single-pulse excitation (repump pulse blocked) by using two chopper wheels. Parallel polarization of the UV pump and 810-nm repump radiation was used in the measurements presented here.

The investigated samples are solutions of NaF, NaCl, NaBr, NaI, and KOH (Merck Eurolab, GR for analysis) solved in de-ionized water at solute concentrations of 1 M, and 80 mM, 5 mM, 5 mM, and 80 mM, respectively. Because of the small two-photon absorption coefficient of the aqueous fluoride

and the lower experimental resolution of the CPM laser system [21] a concentrated solution of 1 M NaF in water was studied in the 310-nm experiment. The studied liquids are circulated in a 100- $\mu\text{m}$  free-flow sample jet (NaBr, NaI, and KOH) or in a 250- $\mu\text{m}$ -thick flow sample cell (NaF, NaCl, and NaI), equipped with 1-mm windows of UV-grade fused silica. In order to maintain a constant sample temperature, the solution passes a heat exchanger and the solvent temperature was controlled via electronic contact thermometer right before the jet/sample cell. Because of the large quantity of the circulated liquid volume (500 ml), the concentration of undesired photo-products like  $\text{Br}_2^-$  [28] can be neglected. Fresh samples were prepared for every experimental session. All data presented here are measured at room temperature.

## RESULTS AND DISCUSSION

Examples for pump–probe signal transients measured in aqueous bromide solution are depicted in Fig. 1. The sample is excited in the first CTTS state at 202 nm (6.15 eV) [29]. The induced absorption changes  $\Delta\text{OD}$  are shown for three characteristic probe wavelengths of 580, 700, and 931 nm (experimental points, calculated solid curves). For convenience, the delay time is plotted on a linear scale up to 2 ps, and on a logarithmic scale for larger values. A rapid, short-lived absorption increase is measured in the mid-infrared that decays close to experimental time resolution (data not shown). This initial absorption narrows significantly and moves to shorter wavelengths with a time constant of about 0.2 ps [22]. The process is assigned to solvent reorganization around the modified charge distribution. The following thermalization of the solvent cavity occurs within the first picosecond (partially seen on the signal transient taken at 931 nm). Accordingly, the absorption increase measured in the visible spectral range is somehow delayed. Especially, for probing at 580 nm the maximum is reached at pump–probe delay time  $t_{13} \sim 1.5$  ps. Analysis of the data in Fig. 1 shows that the changes of the absorption band shape terminate approximately 2–3 ps after the UV excitation, when the well-known spectrum of the hydrated electron has been established [22]. The observed signal decay by a factor of approximately 2.5 within 300 ps is assigned to recombination processes of the detached electrons. The data suggest at least two (effective) time constants involved in the recombination dynamics. The finding is explained by the formation of a precursor, an electron-donor pair that is stabilized by a weak attractive interaction [7,8,18,19].

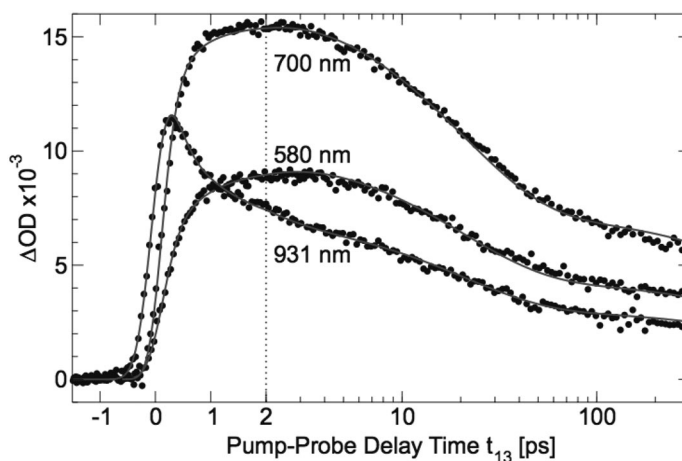


**Fig. 1** Time-resolved absorption changes measured in aqueous bromide solutions after electron photodetachment at 202 nm. Note that the delay time is on a linear scale up to 2 ps, and on logarithmic scale for larger values.

The recombination of the suggested electron-donor pairs is studied using PREP spectroscopy. The technique allows an optical manipulation of the electron relaxation pathway [23] and provides insight in the involved relaxation channels [25,26]. The pulse sequence and the definitions of repump delay  $t_{12}$  and probe delay  $t_{23}$  are illustrated by the inset of Fig. 2. An 810-nm repump pulse is used for secondary excitation of partially and fully released electrons at various delay times after the UV pump at 202 nm. The repump wavelength is suitable for selective interaction with the electrons, since neither the solvent nor the halide anions or neutrals have a significant absorption in this spectral range. Figure 2 shows the PREP data (difference of probe absorption changes induced by repump excitation relative to single-pulse excitation, for details, see ref. [22]) measured at 700 nm for aqueous bromide in a large probe delay interval. The probe absorption rise observed 150 fs after re-excitation is a fairly good measure of the repump-induced number increase of fully solvated electrons  $e^-_{\text{hyd}}$  that escape the recombination process.

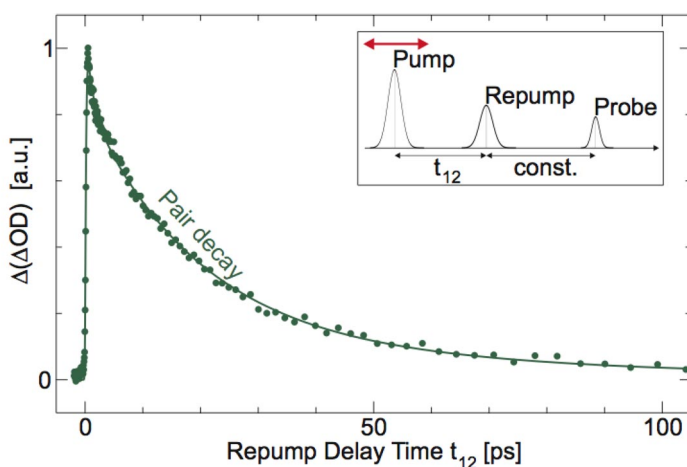


**Fig. 2** PREP signal transients measured at 700 nm in aqueous bromide. Experimental points, calculated solid line. Pulse sequence and definition of delay times used in the PREP experiments are illustrated in the inset. The pump pulse is at 202 nm, whereas the secondary excitation is achieved with 810-nm pulses. The probe signal is measured 150 ps after the repump pulse.

The excitation of a hydrated electron with an 810-nm pulse is followed by rapid relaxation of its solvent environment. The deposited photon energy leads to a significant local heating and so to higher electron mobility [30]. The local temperature jump disappears within 1–2 ps [31]. The fast thermalization may restrict the additional spatial separation of the electron from the parent atom to only a few angstroms. However, this increase of the electron-donor distance is sufficient to convert the pairs into diffusing long-lived electrons and neutral donor atoms in separate solvation shells. The repumping feature gives experimental evidence for the formation of donor-electron pairs separated most likely by one water molecule. Molecular dynamics (MD) simulations on the chloride CTTS system [7,8] and more recent experiments on aqueous iodide [19] report similar results for the halogen-electron separation. Here the question about the special role of this water molecule arises that obviously hinders fast geminate recombination of the pair. In a recent study on aqueous bromide, Elles et al. [28] obtained strong evidence for the generation of a stable Br–H<sub>2</sub>O complex during the electron photodetachment. It may be surmised that this complex plays a role for maintaining a longer-lived ( $\sim 10$  ps) bromine-electron pair. From the PREP signal decay in Fig. 2 (see solid line), exponential time constant  $\tau_{\text{pair}} = 19 \pm 2$  ps is directly determined for aqueous bromide and interpreted as the effective lifetime of the bromine-electron species.

It is interesting to investigate the electron detachment mechanisms for different excitation conditions. The UV absorption spectrum of an aqueous iodide solution [32] is illustrated in the inset of Fig. 3. The figure shows two well-separated CTTS bands centered around 5.5 and 6.4 eV, respectively. The relaxation dynamics measured at 700 nm after excitation at 5.1 eV (242 nm), 6.15 eV (202 nm), and 6.4 eV (194 nm) are presented in Fig. 3. The signal transients indicate a strong increase of the electron survival probability going from 5.1 to 6.15 eV, whereas the relaxation dynamics measured after excitation at 6.15 and 6.4 eV are almost identical. The observation agrees with the recent study by Chen and Bradforth [19] on various CTTS systems. However, it is important to note that the extracted pair time constants are almost the same ( $21 \pm 2$  ps) for the different pumping conditions. The finding gives evidence that an additional relaxation channel for hydrated electrons is opened for excitation in the second CTTS band, while the discussed indirect pathway is not significantly affected. Obviously, the electron detachment from the higher CTTS level involves two channels: (i) the indirect channel involving formation of donor-electron pairs with subsequent electron separation, and (ii) direct ejection of electrons into the solvent. The two pathways are in accordance with theoretical results on the iodide CTTS system [5,6]. Comparing the long-time survival probabilities, the quantum yield of the direct channel after excitation into the second CTTS state is inferred to be  $0.2 \pm 0.05$ . The finding may be related to the larger spatial extension of the CTTS wave function at higher energy, enabling the direct electron ejection [4,26].

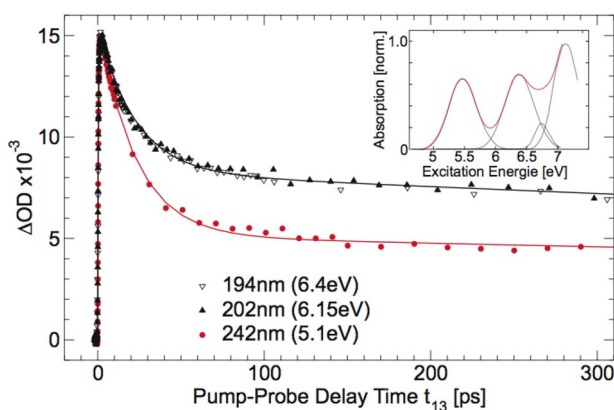


**Fig. 3** Time-resolved absorption changes measured in aqueous iodide solutions at 700 nm after excitation at 242 nm (filled points), 202 nm (filled triangles), and 194 nm (hollow triangles). The UV absorption spectrum of an aqueous iodide solution [32] is shown in the inset. Experimental points, calculated solid lines.

Of special interest is a comparison of the relaxation dynamics of different CTTS systems. Figure 4 compiles data on the electron photodetachment of the four halides ( $F^-$ ,  $Cl^-$ ,  $Br^-$ , and  $I^-$ ) together with that of aqueous hydroxide after resonant excitation into the lowest CTTS state of the respective anion [2,3,20,21]. The selected probe wavelength of 700 nm is close to the absorption maximum of the solvated electron. For better comparison, the signal transients are normalized to the induced absorption measured in aqueous bromide solution at  $t_{13} = 2$  ps. In this way, the initial solvation dynamics and possible ultrafast internal conversion to the anion ground state (reported for  $OH^-$  [33] and  $F^-$  [21]) are excluded from the present discussion. The figure elucidates the dynamics of the electrons on the picosecond time scale after the termination of the thermalization process. The data suggest that the recombination in the CTTS systems presented here exhibits two regimes: (i) a fast approximately exponential decay within tens of picoseconds and (ii) a slower decay that occurs on a sub-nanosecond time scale. The latter is believed to be connected to free diffusive recombination of hydrated electrons and radicals.

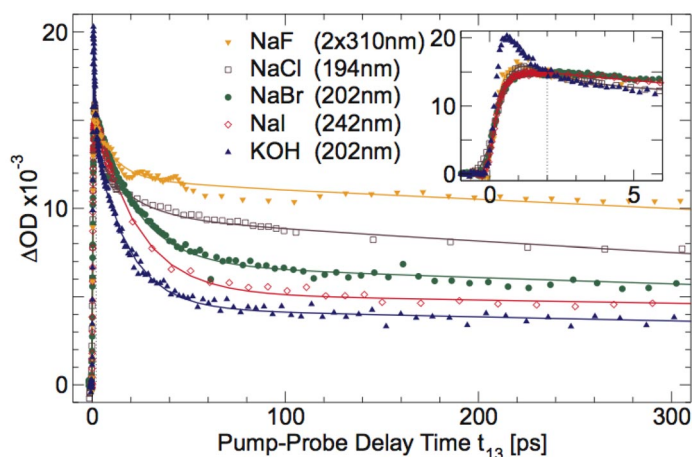


**Fig. 4** Electron photodetachment dynamics measured in NaF, NaCl, NaBr, NaI, and KOH after excitation in the lowest CTTS state of the corresponding anion (see inset). Experimental data measured at 700 nm, calculated solid lines. For better comparison, all traces are normalized to the induced absorption measured in aqueous bromide solution at  $t_{13} = 2$  ps.

Consistent with the discussion above and published theoretical [5–7] and experimental [13–18] studies, the faster decay (i) is assigned to solvent-separated electron-donor pairs. In our simplified relaxation model, the pairs recombine with rate constant  $k_{\text{rec}}$  to ground-state anions or dissociate with rate constant  $k_{\text{dis}}$  to freely diffusing hydrated electrons and radicals. Figure 4 displays a significant spread of the characteristic rate constant  $k_{\text{pair}} = k_{\text{rec}} + k_{\text{dis}}$  and electron survival probability  $\eta_{\text{pair}} = k_{\text{dis}}/k_{\text{pair}}$  of the different samples (see also Fig. 5). The variation cannot be attributed to differences in excitation processes, since all anions are pumped in the first CTTS state with minor excess energy of the detached electrons. The finding suggests a strong influence of the parent radical and supports the conclusion drawn from our PREP data that the excess electron is solvated close to the parent radical, i.e., forms a pair species.

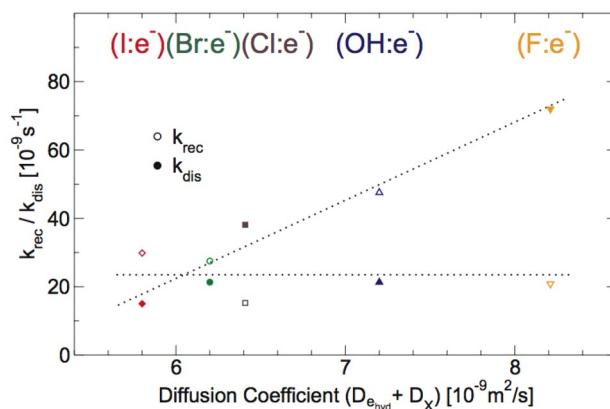


**Fig. 5** Recombination ( $k_{\text{rec}}$ ) and dissociation ( $k_{\text{dis}}$ ) rate constants determined for the pair intermediate vs. mutual diffusion constant (297 K). Note that the OH: $e^-$  pair (black points) does not follow the trend of the halide species (red to orange).

To obtain some insight into the relaxation mechanisms of the electron-donor pairs, the experimental rate constants are compared with the mutual diffusion coefficient of the respective geminate particles [34,35]. The results are depicted in Fig. 5. The pair dissociation rate  $k_{\text{dis}}$  (filled circles) measured in the aqueous halides is seen to increase significantly from  $15 \pm 2$  to  $71 \pm 6 \text{ ns}^{-1}$  going from  $\text{I}^-$  to  $\text{F}^-$  and appears to be proportional to the mutual diffusion coefficient. The finding together with the observed temperature dependence of the recombination dynamics in aqueous iodide and bromide [18,19,22] provides evidence that the pair dissociation is controlled by diffusive motion.

In contrast, the variation of the recombination rate  $k_{\text{rec}}$  measured in these systems is smaller (between  $15 \pm 2$  and  $30 \pm 3 \text{ ns}^{-1}$ ) and does not display a clear correlation with the mutual diffusion coefficient. It should be noted that the relaxation rates determined in aqueous hydroxide do not follow the behavior of the halides (see Fig. 5).

## CONCLUSIONS

The electron photodetachment of the four aqueous halides ( $\text{F}^-$ ,  $\text{Cl}^-$ ,  $\text{Br}^-$ , and  $\text{I}^-$ ) and  $\text{OH}^-$  is studied on the picosecond time scale. The electron release is achieved by excitation into the lowest CTTS state of the corresponding anion, while the recombination dynamics is monitored close to the peak of the absorption band of the generated hydrated electrons. The relaxation of the initial excited state leads to the formation of an intermediate species assigned to a solvent-separated donor-electron pair. The subsequent dynamics is governed by equilibration, recombination and formation of the final, long-lived hydrated electrons. The intermediate is verified in aqueous bromide using PREP spectroscopy.

The geminate decay kinetics for the electrons is bimodal, with a faster exponential component and a slower tail assigned to diffusive motion of the electrons on the sub-nanosecond time scale. The fast decay shows a remarkable influence of the parent radical. The resulting electron escape probability  $\eta_{\text{pair}}$  out of the pair intermediate decreases significantly from  $0.77 \pm 0.02$  to  $0.29 \pm 0.02$  going from  $\text{F}^-$  to  $\text{OH}^-$ . The extracted dissociation rate of the halogen-electron pair seems to be proportional to the mutual diffusion coefficient of the geminate particles, while a correlation between the recombination rate and the diffusion coefficient was not found. The relaxation dynamics of the pair intermediate in aqueous hydroxide solution does not follow this behavior of the halide systems. For  $\text{I}^-$ , the excitation to a higher-lying CTTS state at 6.15 eV opens an additional relaxation channel that directly leads to fully detached, hydrated electrons, while the indirect pathway via the pair intermediate seems to be rather unchanged. The contribution of the direct channel to the quantum yield of hydrated electrons was measured to be  $0.21 \pm 0.05$ .

## REFERENCES

1. B. C. Garrett, D. A. Dixon, D. M. Camaioni, D. M. Chipman, M. A. Johnson, C. D. Jonah, G. A. Kimmel, J. H. Miller, T. N. Rescigno, P. J. Rossky, S. S. Xantheas, S. D. Colson, A. H. Laufer, D. Ray, P. F. Barbara, D. M. Bartels, K. H. Becker, K. H. Bowen Jr., S. E. Bradforth, I. Carmichael, J. V. Coe, L. R. Corrales, J. P. Cowin, M. Dupuis, K. B. Eisenthal, J. A. Franz, M. S. Gutowski, K. D. Jordan, B. D. Kay, J. A. LaVerne, S. V. Lymar, T. E. Madey, C. W. McCurdy, D. Meisel, S. Mukamel, A. R. Nilsson, T. M. Orlando, N. G. Petrik, S. M. Pimblott, J. R. Rustad, G. K. Schenter, S. J. Singer, A. Tokmakoff, L.-S. Wang, C. Wittig, T. S. Zwier. *Chem. Rev.* **105**, 355 (2005).
2. M. J. Blandamer, M. F. Fox. *Chem. Rev.* **70**, 59 (1970).
3. N. Takahashi, K. Sakai, H. Tanida, I. Watanabe. *Chem. Phys. Lett.* **246**, 183 (1995).
4. S. E. Bradforth, P. Jungwirth. *J. Phys. Chem. A* **106**, 1286 (2002).
5. W. S. Sheu, P. J. Rossky. *Chem. Phys. Lett.* **202**, 186 (1993).
6. W. S. Sheu, P. J. Rossky. *J. Phys. Chem.* **100**, 1297 (1996).
7. D. Borgis, A. Staib. *J. Chem. Phys.* **104**, 4776 (1996).

8. A. Staib, D. Borgis. *J. Chem. Phys.* **104**, 9027 (1996).
9. F. H. Long, X. Shi, H. Lu, K. B. Eisenthal. *J. Phys. Chem.* **98**, 7252 (1994).
10. Y. Gauduel, H. Galabert, M. Ashokkumar. *Chem. Phys.* **197**, 167 (1995).
11. M. Assel, R. Laenen, A. Laubereau. *Chem. Phys. Lett.* **289**, 267 (1998).
12. E. R. Barthel, I. B. Martini, B. J. Schwartz. *J. Chem. Phys.* **112**, 9433 (2000).
13. J. A. Kloepfer, V. H. Vilchiz, V. A. Lenchenkov, S. E. Bradforth. *Chem. Phys. Lett.* **298**, 120 (1998).
14. J. A. Kloepfer, V. H. Vilchiz, V. A. Lenchenkov, X. Chen, S. E. Bradforth. *J. Chem. Phys.* **117**, 766 (2002).
15. M. C. Sauer Jr., R. A. Crowell, I. A. Shrob. *J. Phys. Chem. A* **108**, 5490 (2004).
16. M. C. Sauer Jr., I. A. Shrob, R. Lian, R. A. Crowell, D. M. Bartels, X. Chen, D. Suffern, S. E. Bradforth. *J. Phys. Chem. A* **108**, 10414 (2004).
17. R. Lian, D. A. Oulianov, R. A. Crowell, I. A. Shkrob, X. Chen, S. E. Bradforth. *J. Phys. Chem. A* **110**, 9071 (2006).
18. H. Iglev, A. Trifonov, A. Thaller, I. Buchvarov, T. Fiebig, A. Laubereau. *Chem. Phys. Lett.* **403**, 198 (2005).
19. X. Chen, S. E. Bradforth. *Annu. Rev. Phys. Chem.* **59**, 203 (2008).
20. M. Fox, R. McIntyre. *Faraday Discuss.* **64**, 167 (1977).
21. H. Iglev, R. Laenen, A. Laubereau. *Chem. Phys. Lett.* **389**, 427 (2004).
22. M. K. Fischer, A. Laubereau, H. Iglev. *Phys. Chem. Chem. Phys.* **11**, 10939 (2009).
23. I. B. Martini, E. R. Barthel, B. J. Schwartz. *Science* **293**, 462 (2001).
24. A. E. Bragg, M. C. Cavanagh, B. J. Schwartz. *Science* **321**, 1817 (2008).
25. I. B. Martini, B. J. Schwartz. *Chem. Phys. Lett.* **360**, 22 (2002).
26. I. B. Martini, E. R. Barthel, B. J. Schwartz. *J. Am. Chem. Soc.* **124**, 7622 (2002).
27. A. Trifonov. Private communications.
28. C. G. Elles, I. A. Shrob, R. A. Crowell, D. A. Arms, E. C. Landahl. *J. Chem. Phys.* **128**, 061102 (2008).
29. M. Fox, E. Hayon. *J. Chem. Soc., Faraday Trans.* **73**, 872 (1977).
30. K. H. Schmidt, P. Han, D. M. Bartels. *J. Phys. Chem.* **96**, 199 (1992).
31. A. Thaller, R. Laenen, A. Laubereau. *Chem. Phys. Lett.* **398**, 459 (2004).
32. M. Fox, E. Hayon. *J. Chem. Soc., Faraday Trans.* **72**, 344 (1976).
33. R. Petersen, J. Thogersen, S. K. Jansen, S. R. Keiding. *J. Phys. Chem. A* **111**, 11410 (2007).
34. S. Koneshan, J. C. Rasaiah, R. M. Lynden-Bell, S. H. Lee. *J. Phys. Chem. B* **102**, 4193 (1998).
35. M. A. Hervé de Penhoat, T. Goulet, Y. Frongillo, M. J. Fraser, J. P. Jay-Gerin. *J. Phys. Chem. A* **104**, 11757 (2000).